Pergamon

Tetrahedron: *Asymmetry* 10 (1999) 2153–2164

TETRAHEDRON: *ASYMMETRY*

Chiroptical properties of 12,15-dichloro[3.0]orthometacyclophane — correlations between molecular structure and circular dichroism spectra of a biphenylophane

Christoph Niederalt,[a] Stefan Grimme,[a,*] Sigrid D. Peyerimhoff,[a] Adam Sobanski,[b] Fritz Vögtle,[b] Martin Lutz,[c] Anthony L. Spek,[c] Maurice J. van Eis,[d] Willem H. de Wolf [d] and Friedrich Bickelhaupt [d,*]

[a] *Institut für Physikalische und Theoretische Chemie, Universität Bonn, Wegelerstraße 12, D-53115 Bonn, Germany*

[b] *Kekulé-Institut für Organische Chemie und Biochemie, Universität Bonn, Gerhard-Domagk Straße 1, D-53121 Bonn, Germany*

[c] *Bijvoet Center for Biomolecular Research, Department of Crystal and Structural Chemistry, Utrecht University, Padualaan 8, 3584 CH Utrecht, The Netherlands*

[d] *Scheikundig Laboratorium, Vrije Universiteit, De Boelelaan 1083, NL-1081 HV, Amsterdam, The Netherlands*

Received 27 April 1999; accepted 2 June 1999

Abstract

The valence excited electronic states and the circular dichroism (CD) spectra of the recently synthesized 12,15-dichloro[3.0]orthometacyclophane **1** are discussed by means of quantum chemical calculations which combine density functional theory with the single-excitation configuration interaction approach (DFT/SCI). The X-ray structure of this highly strained biphenylophane is presented. In order to investigate the influence of the cyclophane-type distortions on the CD spectrum of **1**, the CD spectra of three model geometries (**2a**–**2c**) are also calculated. It appears that the CD spectrum of the biphenylophane **1** differs substantially from that of the corresponding unstrained biphenyl **2c**. Furthermore, it is found that the pyramidalization of the bridging atoms of the cyclophane ring is an important factor for the red shift of the first band with respect to that of an unstrained benzene chromophore.

1. Introduction

The circular dichroism (CD) spectra of cyclophanes, e.g. ring substituted [2.2]paracyclophanes[1] and [*n*]paracyclophanes,[2,3] hetera[2.2]metacyclophanes[4] and triphenylenicene,[5] have been the subject of

* Corresponding authors. S.G.: Fax: +49 (0)228 739066; e-mail: grimme@rs3b.thch.uni-bonn.de; F.B.: +3120 44 47488; e-mail: bickhpt@chem.vu.nl

0957-4166/99/$ - see front matter
PII: S0957-4166(99)00220-7

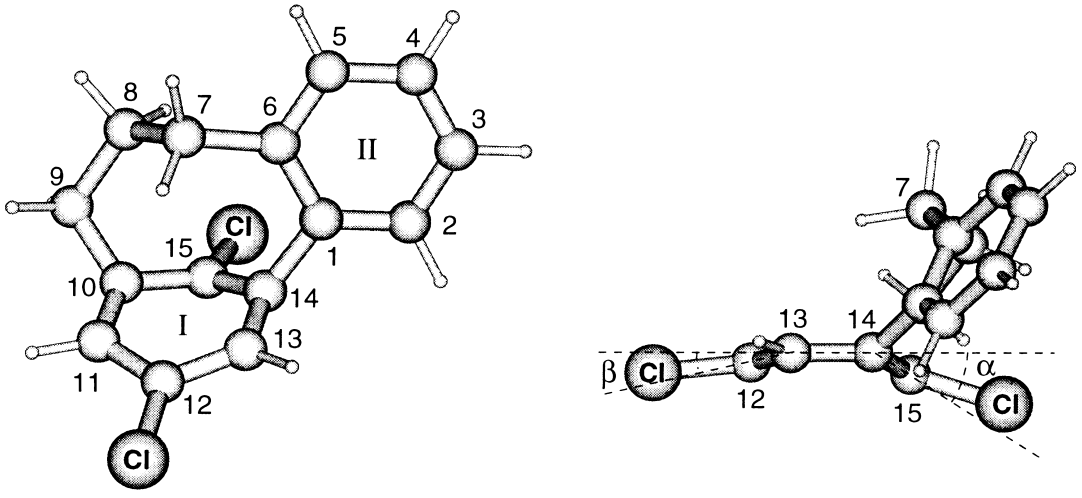

Figure 1. Structure of (*aS*)-*endo*-12,15-dichloro[3.0]orthometacyclophane **1**

special interest. Recently, in the quest for highly strained yet isolable [*n*]metacyclophanes, the synthesis and reactivity of 12,15-dichloro[3.0]orthometacyclophane **1** (see Fig. 1) has been described.[6]

This molecule can be derived from 8,11-dichloro[5]metacyclophane by formally replacing two methylene groups of the cyclophane bridge by an *ortho*-substituted benzene ring. Thereby the structural features of a biphenyl and an [*n*]metacyclophane are combined in this highly strained molecule: the dichloro-substituted benzene ring (atoms C(10)–C(15), henceforth denoted as ring I) shows the typical boat-type distortions of [*n*]metacyclophane, whereas the *ortho*-substituted benzene ring (atoms C(1)–C(6), henceforth denoted as ring II) is only slightly distorted except for the elongation of the C(1)–C(6) bond (see below). Since ring II is incorporated into the cyclophane bridge, the biphenyl axis is strongly bent from linearity. The biphenylophane **1** can be considered as having axial or, depending on the point of view, planar chirality. In the present context, the absolute conformation of **1** is always denoted with reference to the axial chirality of the biphenyl moiety.

In the present paper we discuss the CD spectrum of **1**. Quantum chemical calculations of the CD spectrum have been carried out in order to assign the measured bands and to determine the absolute conformation of **1**. Furthermore, we want to compare the chiroptical properties of the strongly distorted biphenyl moiety of **1** with those of unstrained biphenyls whose chiroptical properties have been studied earlier by several authors.[7–13] For this purpose we have calculated the CD spectra for different geometries of a model system (see Fig. 2).

In this model system the cyclophane bridge is broken in order to change the geometry from that corresponding to the framework of **1** (geometry **2a**) to that of the unstrained biphenyl **2c**. It will be seen that the CD spectrum of the biphenylophane **1** differs substantially from the CD spectrum of the corresponding biphenyl.

2. Experimental details

The preparation of **1** was performed as described previously.[6] Subsequently **1** was separated into its enantiomers using high performance liquid chromatography (HPLC) on a chiral stationary phase (cellulose-tris(3,5-dimethylphenyl)carbamate on silica gel); although failing in baseline separation, the enantiomers could be enriched.

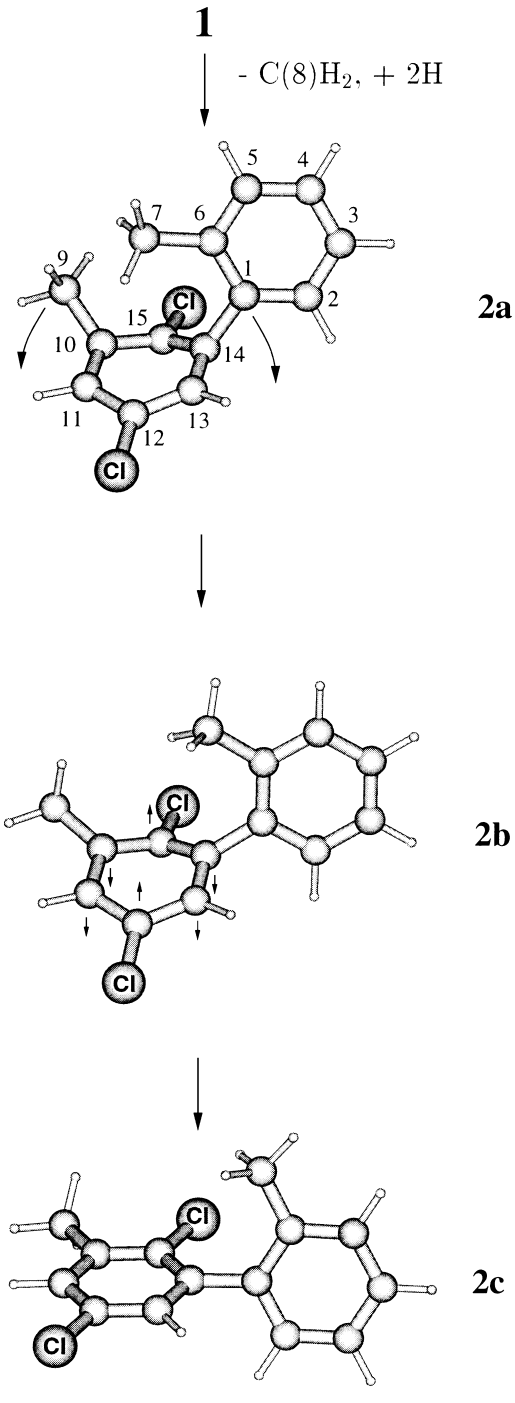

Figure 2. Model geometries of **2a**–**2c**. The most important changes of the geometry from **2a** to **2b** are indicated by arrows (see text)

3. Computational details

The CD spectra (excitation energies and rotatory strengths) were calculated with a recently developed method[14] combining Kohn–Sham density functional theory (DFT) with the single-excitation configuration interaction (SCI) approach. The DFT calculations were performed employing the hybrid B3LYP exchange-correlation functional.[15,16] The Gaussian AO basis sets employed were of split-valence (SV) quality (i.e. [3*s*2*p*] for carbon, [4*s*3*p*] for chlorine and [2*s*] for hydrogen),[17] augmented with polarization *d*-functions at the carbon atoms (exponent α_d=0.8) and at the chlorine atoms (α_d=0.65). This basis set is abbreviated as SV(P). Diffuse Rydberg functions were not included in the AO basis sets because Rydberg transitions are obliterated under the conditions of the measurements in the condensed phase. In the SCI treatment all valence electrons and all virtual MOs were included. The transition moments were calculated in the dipole length form; the origin of the coordinate system lying at the centre of mass of the molecule. The calculated excitation energies correspond to vertical transitions, i.e. the ground state geometry was used for ground and excited states. The rotatory strengths R were given in CGS units, i.e. in esu cm erg G^{-1} which corresponds to 3.336×10^{-15} C^2 m^3 s^{-1} in SI units. The simulated CD spectra were obtained by summing up Gaussian curves weighted with the calculated rotatory strengths.[18] For all molecules and transitions, the width of the Gaussian curves (full width of half maximum) was chosen to be 0.33 eV.

The molecular geometries of **1** and **2a**–**2c** were calculated with the PM3-Hamiltonian.[19] The molecular geometry of **1** was also calculated at the ab initio RI-MP2 level of treatment.[20] In the RI-MP2 method, an approximate resolution of identity (RI) is used to calculate the MP2 energy and its first derivatives. For the RI-MP2 calculations, an SVP basis was employed, i.e. the SV(P) basis set was additionally augmented with a polarization *p*-function at the hydrogen atoms (α_p=0.8); the auxiliary basis set used is the same as in the literature.[20] The DFT and RI-MP2 calculations are performed with the TURBOMOLE suite of programs[21,22] and the PM3 calculations with the MOPAC 6.0[23] program system.

4. Results and discussion

*4.1. Geometry of the biphenylophane **1***

The X-ray data indicate that **1** adopts the *endo* conformation (atom C(7) points toward C(12), see Fig. 3). This confirms previous density functional results[6] indicating that the *endo* conformation is preferred over the *exo* conformation by 3.3 kcal/mol. Selected experimental geometrical parameters of *endo*-**1** are compared with calculated ones obtained at the PM3 and the RI-MP2 level of treatment in Table 1.

The most pronounced deformations of ring II with respect to benzene occur in the strong elongation of the bond C(1)–C(6) and in the bond angles of C(6). In the experimental structure, the bond C(3)–C(4) is somewhat shortened which is not reflected by any of the present calculations. Ring I adopts an unsymmetrical boat-like conformation; i.e. the atoms C(12) and C(15) are distorted out of the plane of the remaining benzene carbon atoms. For the deformation angles α and β (angle between plane C(10)C(11)C(13)C(14) and C(10)C(15)C(14) and between plane C(10)C(11)C(13)C(14) and C(11)C(12)C(13), respectively, see Fig. 1) values of α=26.8(2)° and β=12.1(1)° were found (X-ray data). A further distortion of ring I results from the pyramidalization of especially the bridging atoms C(10) and C(14). According to the crystal structure analysis, the sum of the bond angles for these atoms is 354.9° and 353.9°, respectively, whereas values from 357.4° (for C(15)) to 360° were obtained for the other carbon atoms of ring I. The strain of the molecule also became evident in the elongation of

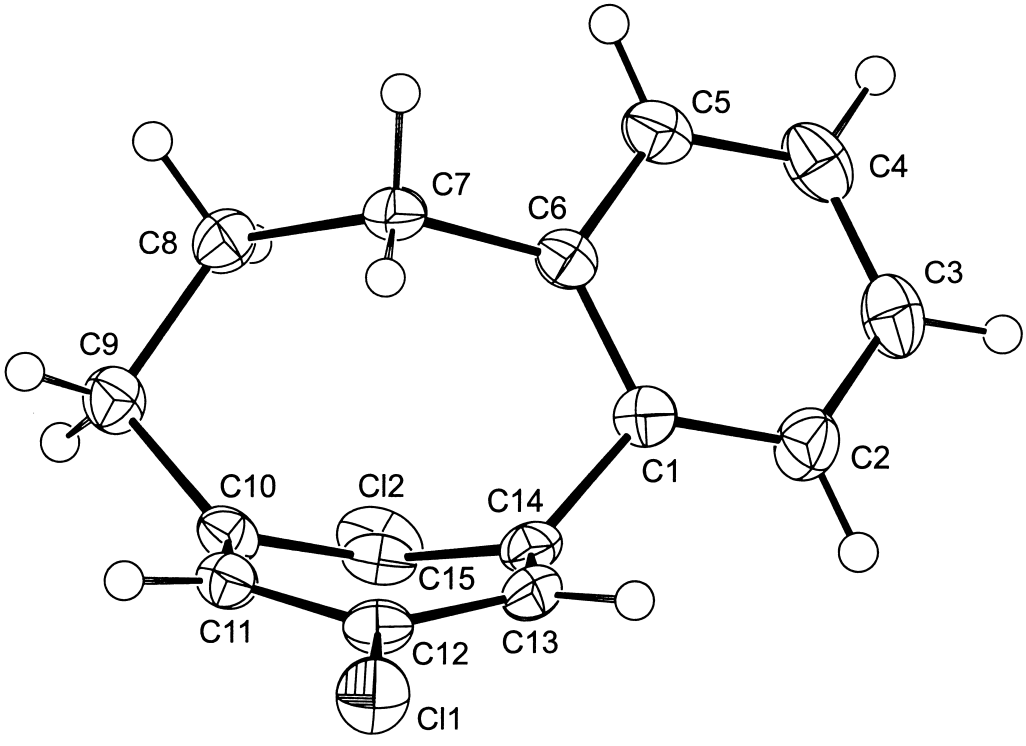

Figure 3. Crystal structure of *endo*-12,15-dichloro[3.0]orthometacyclophane **1**. Displacement ellipsoid plot (50% probability)

most of the bonds and in the distortion of most bond angles in the cyclophane bridge. The torsion angles along C(1)–C(14) have four different values because of the boat-type distortion of ring I (Table 1). The geometry obtained at the RI-MP2 level of treatment is in very good agreement with the crystal structure. The largest deviation occurs in the bond length C(3)–C(4), as mentioned above. The X-ray data also confirm the density functional values for the geometrical parameters published in the literature.[6] The most pronounced difference between the X-ray data and the density functional data lies in the distance between the cyclophane bridge and the cyclophane ring, e.g. in the non-bonded distance C(7)–C(15) of *endo*-**1**. This distance is overestimated by the density functional calculations: 2.862 Å compared to 2.818(3) Å according to the X-ray data. Although the density functional and RI-MP2 values are generally in very good agreement, the C(7)–C(15) distance obtained by the RI-MP2 method is in considerably better agreement with the X-ray data. An analogous deviation of density functional calculations from X-ray data and RI-MP2 calculations was also found in the case of the inter-ring distance of [2.2]metacyclophanes[24] and an azulenophane.[25]

The geometry of **1** obtained at the PM3 level of treatment is generally also in good agreement with the X-ray data. Larger deviations occur for the C–C bond lengths of the cyclophane bridge and the central biphenyl bond C(1)–C(14) which are calculated to be 1.9 to 4.2 pm too short at the PM3 level of theory, the largest deviation occurring for the elongated bond C(7)–C(8). The deformation angles are somewhat overestimated at the PM3 level of treatment: values of α=31.3° and β=13.3° are obtained at the PM3 level compared to α=26.8(2)° and β=12.1(1)° from the X-ray data. Since the CD spectrum calculated with the PM3 geometry is in good agreement with the experimental CD spectrum all further calculations of CD spectra are based on geometries calculated with the PM3-Hamiltonian.

Table 1
Comparison of selected experimental and calculated geometrical parameters of **1**. Distances are given in Å, angles in degrees

		PM3	RI-MP2/SVP	X-ray
	C(1)-C(6)	1.419	1.431	1.421(2)
ring II	C(3)-C(4)	1.388	1.399	1.378(3)
(C(1) – C(6))	remaining four C-C lengths	1.388 - 1.394	1.399 - 1.404	1.392(2) - 1.399(2)
	C(1)-C(6)-C(5)	117.8	117.2	117.4(1)
	remaining five C-C-C angles	119.7 - 221.2	119.7 - 121.6	119.8(2) - 121.1(2)
ring I	C-C bond lengths	1.392 - 1.407	1.400 - 1.406	1.385(2) - 1.397(2)
(C(10) – C(15))	C-C-C angles	114.6 - 119.7	117.5 - 119.8	116.6(2) - 120.3(2)
	C(6)-C(7)	1.516	1.537	1.548(2)
	C(7)-C(8)	1.541	1.570	1.582(2)
	C(8)-C(9)	1.553	1.573	1.579(2)
cyclophane	C(9)-C(10)	1.492	1.507	1.511(2)
bridge	C(6)-C(1)-C(14)	114.6	112.2	112.6(1)
	C(1)-C(6)-C(7)	123.7	123.7	124.2(1)
	C(6)-C(7)-C(8)	117.7	120.7	121.0(2)
	C(7)-C(8)-C(9)	117.1	118.1	118.6(1)
	C(8)-C(9)-C(10)	108.9	108.3	108.5(1)
	C(1)-C(14)	1.469	1.482	1.498(2)
	C(7)-C(15)	2.860	2.803	2.818(3)
	α	31.3	25.6	26.8(2)
	β	13.3	10.9	12.1(1)
pyramidalization	C(10)	356.2	354.5	354.9
(sum of bond angles)	C(14)	355.5	353.5	353.9
	C(2)-C(1)-C(14)-C(13)	81.5	87.8	86.8(2)
	C(2)-C(1)-C(14)-C(15)	-122.8	-121.1	-121.4(2)
	C(6)-C(1)-C(14)-C(13)	-100.1	-95.4	-97.6(2)
	C(6)-C(1)-C(14)-C(15)	55.6	55.7	54.2(2)

4.2. Chiroptical properties

The experimental and calculated CD spectra of **1** are compared in Fig. 4. In the experimental CD spectrum, four bands (λ_{max}=331, 285, 204 and 185 nm) and one broad band system (217–267 nm, minima at 222 and 254 nm) are seen in the wavelength range down to 180 nm and are denoted A–E. The calculated and experimental CD spectra are generally in good agreement. Compared to the experimental spectrum, the calculated transitions in the long-wavelength range (especially the transition attributed to band B) are red shifted. The calculated CD intensity is generally slightly larger than the experimental one; however, this may be attributed to the incomplete enantioresolution of **1**. Since the calculated CD

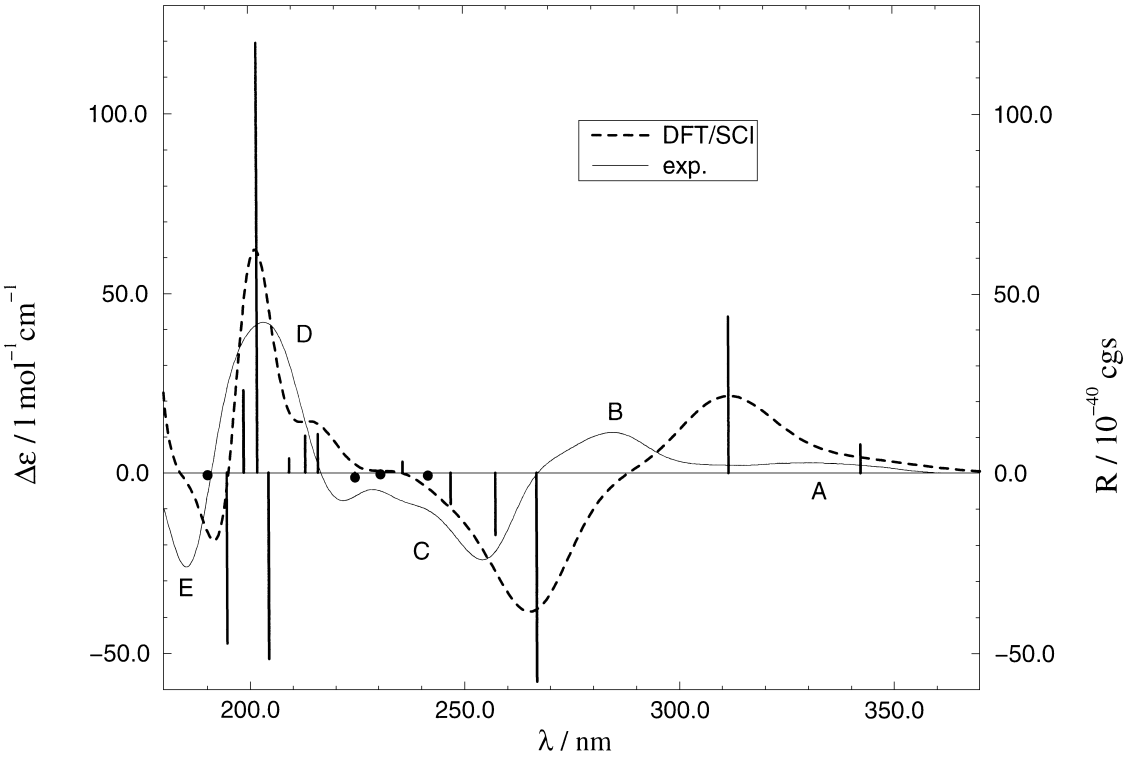

Figure 4. Comparison of the calculated CD spectrum of (*aS*)-*endo*-**1** (dashed line) and the experimental CD spectrum (solid line). The calculated rotatory strengths (R) are designated by sticks, excitations with very small rotatory strengths are indicated with filled circles. The dashed line shows the simulated CD spectrum which is obtained by summing up rotatory strengths weighted Gaussian curves with Δ_{fwhm}=0.33 eV

spectrum shown in Fig. 4 is obtained with a geometry of (*aS*) conformation, this conformation can be assigned to the enantiomer whose CD spectrum is shown in Fig. 4 (positive CD band at 204 nm).

The characterization of the transitions on the basis of the transition densities is given in Table 2. The first two positive CD bands (A and B) can be assigned to L_b and L_a transitions, respectively, which are essentially localized at the cyclophane-type distorted ring I (transitions of this type will be abbreviated by L_b(I) and L_a(I)). The transition density of the L_a(I) state has slightly larger contributions from parts outside ring I, namely from the region of C(1), C(6), C(2) and the bridge atom C(8). The observed L_b(I) band is centred at 331 nm and thereby strongly red shifted with respect to the corresponding transitions in unstrained compounds (compare for example the L_b transition in 1,4-dichlorobenzene which is located at λ_{max}=272 nm).[26] This red shift is also found in other strained [*n*]cyclophanes and is attributed to the distortion of the benzene ring.[27] A transition which is composed of an L_b transition at ring II and a π–π* transition at ring I is calculated at 257 nm, near the position of the L_b band in *o*-xylene at λ_{max}=262 nm.[26] The strong transition calculated at 267 nm is of π–π* character; it is not localized at one of the benzene rings and cannot be traced back to a transition of the benzene chromophore. In the 213–236 nm region, a series of ring-to-ring charge transfer transitions is found. The most intense CD band observed at 204 nm (band D) originates mainly from a transition which is composed of an L_a(II) transition and a lone pair(Cl) → π* transition.

In order to gain further insight into the relationship between molecular structure on the one hand and the character of the excited states and chiroptical properties on the other, we compare the CD spectrum of **1** with those of the different model geometries (**2a**–**2c**) shown in Fig. 2. In the first step, the cyclophane

Table 2
DFT/SCI results for the vertical excitation wavelengths (λ), oscillator strengths (f) and rotatory strengths (R) of (*aS*)-*endo*-**1**. The transitions are characterized according to the nomenclature of Platt[34] whenever possible. If a transition is essentially localized in ring I (C(10)–C(15)) or in ring II (C(1)–C(6)), this is specified in parentheses. A lone pair of a chlorine substituent is abbreviated by lp and a charge transfer transition by CT

state	λ/nm	f	R/cgs	band	character of excited state
$2\,^1$A	342	0.021	8.0	A	^1L_b(I)
$3\,^1$A	312	0.124	43.7	B	^1L_a(I)
$4\,^1$A	267	0.186	-57.7	C	$\pi \rightarrow \pi^*$
$5\,^1$A	257	0.041	-17.3	C	^1L_b(II), $\pi \rightarrow \pi^*$(I)
$6\,^1$A	247	0.014	-8.7	C	$\pi \rightarrow \pi^*$
$7\,^1$A	242	0.056	-0.8	C	$\pi \rightarrow \pi^*$
$8\,^1$A	236	0.025	3.0		$\pi \rightarrow \pi^*$, $CT^{II\rightarrow I}$
$9\,^1$A	231	0.010	-0.5	C	$\pi \rightarrow \pi^*$
$10\,^1$A	225	0.002	-1.4	C	$\pi \rightarrow \pi^*$, $CT^{I\rightarrow II}$
$11\,^1$A	216	0.053	10.7	D	$\pi \rightarrow \pi^*$, $CT^{II\rightarrow I}$
$12\,^1$A	213	0.047	10.3	D	$\pi \rightarrow \pi^*$, $CT^{I\rightarrow II}$
$13\,^1$A	209	0.057	3.9	D	$\pi \rightarrow \pi^*$
$14\,^1$A	204	0.197	-51.6		$\pi \rightarrow \pi^*$
$15\,^1$A	202	0.066	119.4	D	^1L_a(II), $lp(Cl^{15}) \rightarrow \pi^*$, $\pi \rightarrow \pi^*$(I)
$16\,^1$A	199	0.053	22.9	D	$lp(Cl^{15,12}) \rightarrow \pi^*$, ^1L_a(II), $\pi \rightarrow \pi^*$(I)
$17\,^1$A	195	0.086	-47.3	E	$lp(Cl^{15,12}) \rightarrow \pi^*$, $\pi \rightarrow \pi^*$

bridge is broken by removing the methylene group of C(8) and exchanging the methylene groups of C(7) and C(9) with methyl groups. In this way it is possible to change the geometry of **1** to that of an unstrained biphenyl in two further steps (see Fig. 2). In order to test the influence of the variations in the cyclophane bridge on the calculated CD spectrum, the first geometry **2a** was chosen to be exactly the geometry of **1** except for the optimized position of the hydrogen atoms of the methyl groups. The calculated CD spectra of **2a** and **1** are compared in Fig. 5.

The first four calculated transitions of **2a** agree almost exactly in position, rotatory strength and character with those of **1**. In the shorter wavelength region, the influence of the cyclophane bridge becomes larger and more pronounced differences between the calculated CD spectra of **1** and **2a** are observed. At least in the long-wavelength region, the structure **2a** can thus be considered to be well suited as a model system for **1**.

In the next step (geometry **2b**), the pyramidalization of the atoms C(10) and C(14) was removed while the boat-type distortion of ring I was maintained. For this purpose all coordinates were relaxed except those of the six carbon atoms of the benzene ring I and its two chlorine and hydrogen substituents. The pyramidalization of the atoms C(10) and C(14) was explicitly removed during the optimization, since without this additional constrain the pyramidalization would not completely vanish but a slight inverted

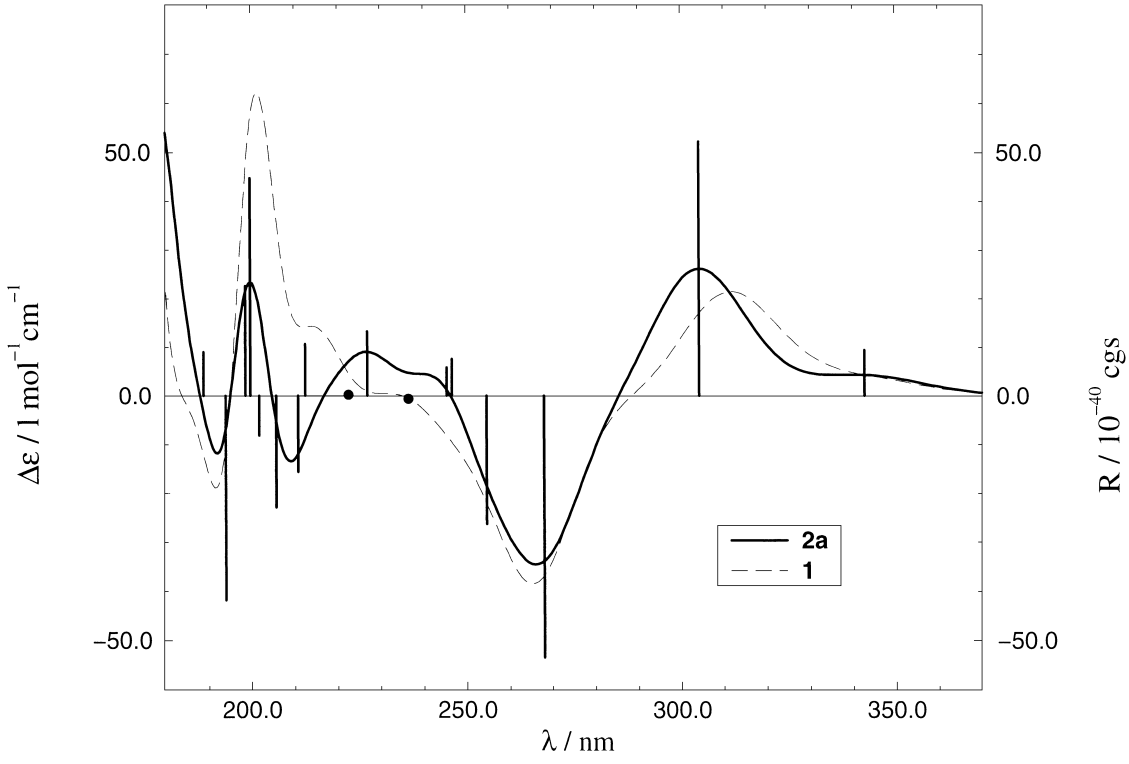

Figure 5. Calculated CD spectrum of the model geometry **2a** (solid line). The simulated CD spectrum of the biphenylophane **1** is given for comparison as a dashed line

pyramidalization would occur. Furthermore, the torsion angle between the two benzene rings was fixed so that the average torsion angle of **2b** equals that of **2a** (and of **1**).

In the structure **2c** all constraints were released except for the average torsion angle between the two benzene rings which equals that of the previous structures **1**, **2a** and **2b**. Structure **2c** thus represents a substituted biphenyl. The simulated CD spectra of **2b** and **2c** are compared with that of **2a** in Fig. 6.

As in the biphenylophane **1**, the first transition of all three model geometries is of L_b(I) character. The position of this band was strongly blue shifted from 343 nm in **2a** to 295 nm in **2b** and blue shifted to a smaller extent to 278 nm in **2c**. Since in **2b** the boat-type distortion of the framework of the carbon atoms in ring I is still present, it appears that the pyramidalization (or rehybridization) of the atoms C(10) and C(14) was an important factor for the red shift of the first transition of the biphenylophane **1** compared to corresponding unstrained molecules. Note that an increase in the conjugation between the two benzene rings would lead to a red shift[10,28] which is possibly superimposed to the calculated blue shift in going from **2a** to **2c**.[†]

The rotatory strength of the L_b(I) transition becomes smaller and changes the sign in going from **2a** to **2b** and is close to zero in **2c**. The second transition of **2a** and **2b**, which shows a large positive Cotton effect, is of L_a(I) character. Also this transition is blue shifted by 25 nm in going from **2a** to **2b**. The second transition of **2c**, on the other hand, is of L_b(II) type with a small L_a(I) contribution and its rotatory

[†] It is only in an arbitrary way possible to remove the deformation angle α and to maintain the pyramidalization of the atoms C(10) and C(14). In a benzene model we have varied both α and the pyramidalization. It turns out that the strong dependence of the red shift of the L_b band on the pyramidalization occurs only if the angle α is large. In other words, the strong red shift of the L_b band occurs only if the angle α as well as the pyramidalization are considerably large.

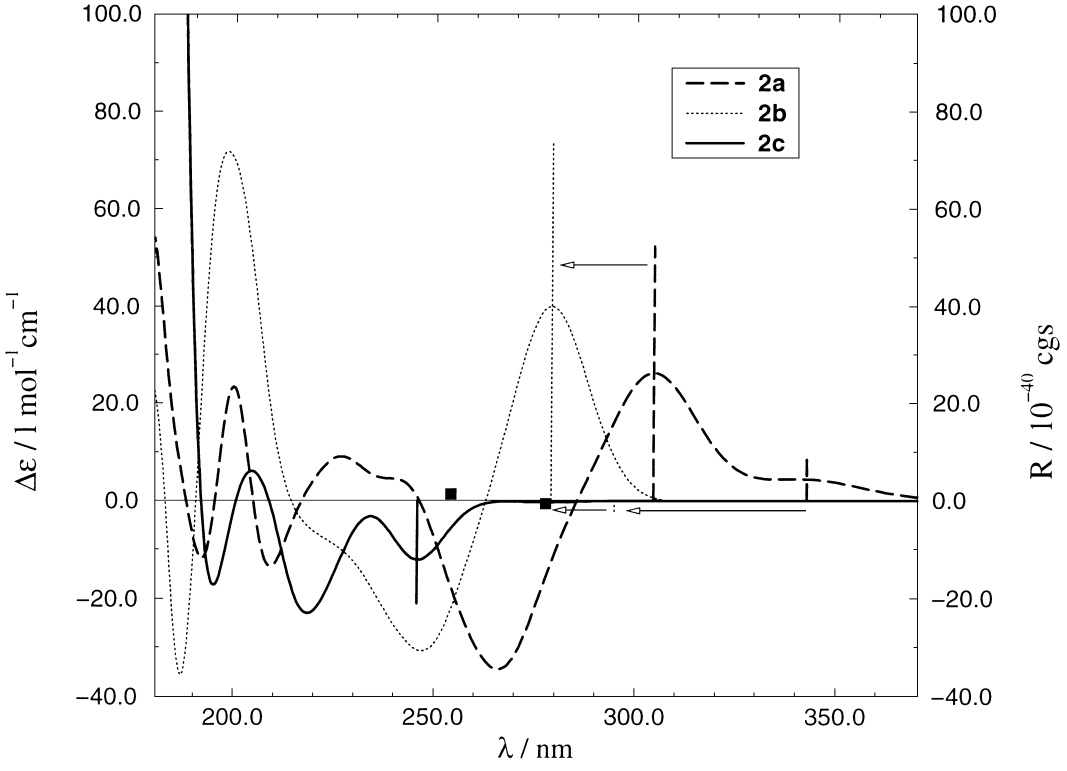

Figure 6. Comparison of the simulated CD spectra of the model geometries **2a**, **2b** and **2c**. Only the positions and rotatory strengths (R) of the first two transitions of **2a** and **2b**, and of the first three transitions of **2c** are designated by sticks. The shift of corresponding transitions is indicated by arrows

strength is close to zero. The broad negative region from 214–263 nm in the spectrum of **2b** is caused by ring-to-ring charge transfer and π–π* transitions. The third transition and first stronger band in the spectrum of **2c** is a combination of the L_a states of the two rings and corresponds thus to the conjugation band of other biphenyls. The sign of this band is known to be characteristic for the absolute conformation of bridged, symmetrically substituted biphenyls, i.e. it is negative for (*aS*)-biphenyls as is also the case for **2c**.[7–10] In the short wavelength limit of the spectrum of **2c**, a very strong positive band occurs which is not found in the CD spectra of **1**, **2a** and **2b**. This band originates from two transitions of which the strongest one, calculated at 183 nm, is due to the coupling of the B_b(I) and B_b(II) transitions.

Although **1** contains a biphenyl moiety, its CD spectrum differs significantly from that of the unstrained biphenyl **2c**. One reason is that ring I shows a boat-type conformation with a pronounced pyramidalization at C(10) and C(14) while ring II is only slightly distorted. As a consequence, the benzene chromophore transitions of ring I are strongly shifted with respect to those of ring II. The transitions found in **1** therefore have a different character than those of **2c** and for example, the 'conjugation band' (combination of the L_a transitions at both rings) occurs in **2c** but not in **1**. Furthermore the cyclophane-type distortions have not only influence on the CD spectrum of **1** by shifting the transition energies of one ring with respect to those of the other ring, but also by affecting the transition moments. The boat-type deformation gives, for example, rise to a magnetic transition moment in the L_a(I) transition. The signs of the several CD bands in the spectrum of **1** are rather difficult to explain since the structure of the chromophore of **1** is much more complex than that of the unstrained biphenyl.

Finally, it should be noted that the energy difference between **2a** and the conformer of **2c** in which the torsion angle between the benzene rings is relaxed, can be considered as strain energy of **1**. By this

approach, a strain energy of 51 kcal/mol is obtained at the PM3 level of theory in good agreement with the value calculated[6] by using group increments (48 kcal/mol).

5. Summary

The DFT/SCI method has been applied in order to discuss the CD spectrum and the valence excited states of the biphenylophane **1**. The absolute conformation has been assigned on the basis of the calculated CD spectrum. By calculating the CD spectra of three model geometries, it was found that the CD spectrum of the biphenylophane **1** differs substantially from that of the corresponding unstrained biphenyl **2c**. Furthermore it was found that the pyramidalization of the bridging atoms C(10) and C(14) is, besides the boat-type deformation, an important factor for the red shift of the transitions localized at the cyclophane-like distorted ring I with respect to those of corresponding unstrained molecules or those of ring II.

6. Experimental

6.1. Crystal structure determination

$C_{15}H_{12}Cl_2$, M_r=263.15 g mol^{-1}, pale yellow needles, 0.82×0.44×0.13 mm^3, orthorhombic, $Pca2_1$, a=16.4769(4) Å, b=10.4623(2) Å, c=7.2599(1) Å, V=1251.51(4) Å^3, Z=4, ρ=1.397 g cm^{-3}, 12 085 measured reflections, 2476 unique reflections (R_{int}=0.0943), R ($I>2\sigma(I)$): $R1$=0.0256, $wR2$=0.0660. R (all data): $R1$=0.0267, $wR2$=0.0669, S=1.052. Intensities were measured on a Nonius Kappa CCD diffractometer with rotating anode (Mo-K$_\alpha$, λ=0.71073 Å) at a temperature of 150 K. The structures were solved with the program SIR97[29] and refined with the program SHELXL97[30] against F^2 of all reflections up to a resolution of $(\sin\theta/\lambda)_{max}$=0.65 Å^{-1}. Non hydrogen atoms were refined freely with anisotropic displacement parameters. Hydrogen atoms were refined as rigid groups. An absorption correction was not considered necessary. The drawings, structure calculations and checking for higher symmetry were performed with the program PLATON.[31] The absolute structure was determined by refinement of the Flack x parameter,[32] which resulted in x=0.00(5).

6.2. Enantioresolution

Chiralcell OD®, cellulose-tris(3,5-dimethylphenyl)carbamate (CDMPC) on silica gel, 250×10 mm; eluent: *n*-hexane; 1.5 mL min^{-1}; injection of 5 μL portions of a 1.9×10^{-5} molar solution of **1** in *n*-hexane; pressure: 17 bar; temp.: 0°C; detection: UV, λ=254 nm; resolution parameter[33] R_{ij}=0.58. CD measurement: JASCO-spectropolarimeter *J* 700; 1.9×10^{-4} mol L^{-1} (enantiomer with positive CD band at 204 nm), 9.56×10^{-5} mol L^{-1} (enantiomer with negative CD band at 204 nm) solution in *n*-hexane (concentration was determined by UV measurements of the enantiomers and calibration with racemic solution), 0.2 mm cell.

Acknowledgements

The services and computer time made available by the Sonderforschungsbereich 334 (‘Wechselwirkungen in Molekülen’) have been essential to this study which was financially supported by the

Deutsche Forschungsgemeinschaft. This investigation was also supported (M.J.v.E., M.L., A.L.S.) by the Council of Chemical Sciences (GCW) with financial aid from the Netherlands Organization for Scientific Research (NWO). S.G. thanks the Land Nordrhein-Westfalen for financial support through the Bennigsen-Foerder-Preis.

References

1. Weigang, O. E.; Nugent, M. J. *J. Am. Chem. Soc*. **1969**, *91*, 4555–4556, 4556–4558.
2. Tochtermann, W.; Vagt, U.; Snatzke, G. *Chem. Ber*. **1985**, *118*, 1996–2010.
3. Tochtermann, W.; Olsson, G.; Mannschreck, A.; Stühler, G.; Snatzke, G. *Chem. Ber*. **1990**, *123*, 1437–1439.
4. Grimme, S.; Peyerimhoff, S. D.; Bartram, S.; Vögtle, F.; Breest, A.; Hormes, J. *Chem. Phys. Lett.* **1993**, *213*, 32–40.
5. Buss, V.; Klein, M. *Chem. Ber*. **1988**, *121*, 89–93.
6. van Eis, M. J.; de Kanter, F. J. J.; de Wolf, W. H.; Bickelhaupt, F. *J. Am. Chem. Soc*. **1998**, *120*, 3371–3375.
7. Mislow, K.; Glass, M. A. W.; O'Brien, R. E.; Rutkin, P.; Steinberg, D. H.; Weiss, J.; Djerassi, C. *J. Am. Chem. Soc*. **1962**, *84*, 1455–1478.
8. Bunnenberg, E.; Djerassi, C.; Mislow, K.; Moscowitz, A. *J. Am. Chem. Soc*. **1962**, *84*, 2823–2826, 5003.
9. Mislow, K.; Bunnenberg, E.; Records, R.; Wellman, K.; Djerassi, C. *J. Am. Chem. Soc*. **1963**, *85*, 1342–1349.
10. Mislow, K.; Glass, M. A. W.; Hopps, H. B.; Simon, E.; Wahl Jr., G. H. *J. Am. Chem. Soc*. **1964**, *86*, 1710–1733.
11. Mason, S. F.; Seal, R. H.; Roberts, D. R. *Tetrahedron* **1974**, *30*, 1671–1682.
12. Seno, K.; Hagishita, S.; Sato, T.; Kuriyama, K. *J. Chem. Soc., Perkin Trans. 1* **1984**, 2013–2022.
13. Rashidi-Ranjbar, P.; Sandström, J. *J. Mol. Struct*. **1991**, *246*, 25–32.
14. Grimme, S. *Chem. Phys. Lett*. **1996**, *259*, 128–137.
15. Becke, A. D. *J. Chem. Phys*. **1993**, *98*, 5648–5652.
16. Stephens, P. J.; Devlin, F. J.; Chabalowski, C. F.; Frisch, M. J. *J. Phys. Chem*. **1994**, *98*, 11623–11627.
17. Schäfer, A.; Horn, H.; Ahlrichs, R. *J. Chem. Phys*. **1992**, *97*, 2571–2577.
18. Schellman, A. *Chem. Rev*. **1975**, *75*, 323–331.
19. Stewart, J. J. P. *J. Comp. Chem*. **1989**, *10*, 209.
20. Weigend, F.; Häser, M. *Theor. Chem. Acc*. **1997**, *97*, 331–340.
21. Ahlrichs, R.; Bär, M.; Häser, M.; Horn, H.; Kölmel, C. *Chem. Phys. Lett.* **1989**, *162*, 165–169.
22. Treutler, O.; Ahlrichs, R. *J. Chem. Phys*. **1995**, *102*, 346–354.
23. Stewart, J. J. P. *QCPE Bull*. **1985**, *5*, 133.
24. Habel, M.; Niederalt, C.; Grimme, S.; Nieger, M.; Vögtle, F. *Eur. J. Org. Chem*. **1998**, 1471–1477.
25. Grimme, S.; Mennicke, W.; Vögtle, F.; Nieger, M. *J. Chem. Soc., Perkin Trans. 2* **1999**, 521–527.
26. *Sadtler Handbook of Ultraviolet Spectra*; Simons, W. W., Ed.; Sadtler Research Laboratories: Philadelphia, PA, 1979.
27. Vögtle, F. *Cyclophane Chemistry*; Wiley: Chichester, 1993.
28. Rubio, M.; Merchán, M.; Ortí, E.; Roos, B. O. *Chem. Phys. Lett*. **1995**, *234*, 373–381.
29. Altomare, A.; Burla, M. C.; Camalli, M.; Cascarano, G. L.; Giacovazzo, C.; Guagliardi, A.; Moliterni, A. G. G.; Polidori, G.; Spagna, R. *J. Appl. Crystallogr*. **1999**, *32*, 115–119.
30. Sheldrick, G. M. *SHELXL-97. Program for Crystal Structure Refinement*; University of Göttingen: Germany, 1997.
31. Spek, A. L. *PLATON. A Multipurpose Crystallographic Tool*; Utrecht University: The Netherlands, 1998.
32. Flack, H. D. *Acta Cryst*. **1983**, *A39*, 876–881.
33. Schmitz, F. P. *J. Chromatogr.* **1986**, *356*, 261–269.
34. Platt, J. R. *J. Chem. Phys*. **1949**, *17*, 484–495.